The Biotin Regulatory System: Kinetic Control of a Transcriptional Switch†

Emily D. Streaker and Dorothy Beckett*

Department of Chemistry and Biochemistry and Center for Biological Structure and Organization, University of Maryland, College Park, Maryland 20742

Received December 20, 2005; Revised Manuscript Received March 17, 2006

ABSTRACT: An organism's response to environmental and metabolic cues requires communication between transcription regulatory processes and "other" cellular events. In a number of biological control circuits, the communication is carried out by a single multifunctional protein that participates directly in transcription initiation and in at least one other cellular process. Structural studies suggest that the function of these proteins is dictated by the formation of mutually exclusive protein−protein interactions. However, the rules that govern partner, and thus functional switching, are not known. In the *Escherichia coli* Biotin Regulatory System, the bifunctional protein, BirA, catalyzes post-translational biotin addition to a biotin-dependent carboxylase and binds sequence-specifically to DNA to repress transcription initiation at the biotin biosynthetic operon. Previous structural and modeling studies suggest that BirA function is determined by formation of alternative homo- and heterodimeric protein−protein interactions. In this work, the BirA functional switch is investigated using DNaseI footprinting and MALDI-TOF mass spectrometry. Results of these measurements indicate that BirA can be selectively targeted toward its enzymatic function simply by increasing the kinetic probability of heterodimerization relative to that of homodimerization. Subsequent shifting to the DNA binding function occurs as the pool of heterodimer partner is depleted and homodimerization dominates. The data support a switching mechanism in which BirA's function is dictated by its probability of encountering a particular protein partner.

Cross talk between diverse cellular processes and gene expression is essential for all organisms. In many cases, this communication occurs *via* the activities of distinct macromolecules. For example, in signal transduction, the extracellular signaling molecule binds to a membrane-bound receptor and, through a series of intracellular phosphoryl-transfer events, the signal ultimately reaches proteins that function directly in transcription initiation. An alternative mechanism for linking "other cellular processes" to transcription is through the action of multifunctional transcription factors. These proteins are active in both transcription initiation and at least one other cellular process. One protein characterized by this versatility is β-catenin, which serves a structural role in adherens junctions and is also a coactivator of transcription initiation (*1*, *2*). Another example is the bacterial protein PutA, which is both a redox enzyme in the proline utilization pathway and a regulator of transcription initiation for the operon that encodes enzymes involved in proline utilization (*3*). Although several of these multifunctional transcription factors have been identified, their mechanisms of functional switching have yet to be elucidated.

The Biotin Regulatory System provides an example of the use of a single protein in metabolic and transcription regulatory roles (Figure 1). In *Escherichia coli*, the protein BirA, which functions as the biotin protein ligase and biotin repressor, is responsible for covalent attachment of biotin to the biotin-dependent carboxylase, acetyl CoA carboxylase

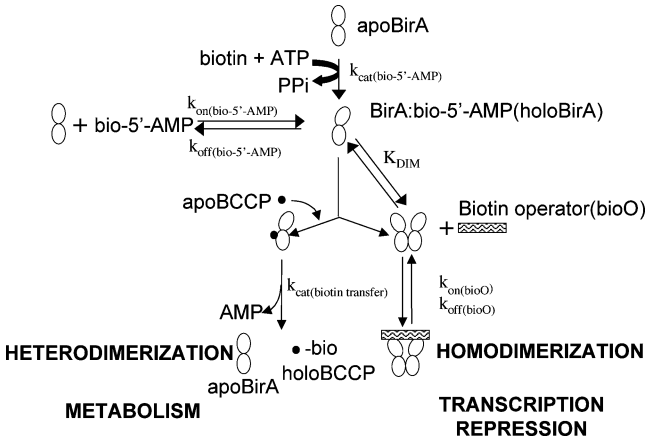

FIGURE 1: Schematic diagram of the Biotin Regulatory System. The Biotin Repressor/Biotin protein ligase, BirA, binds biotin and ATP and catalyzes synthesis of bio-5′-AMP. BirA is shown as two ovals, which represent the N-terminal DNA binding domain and combined central and C-terminal domains. The change in the orientations of the domains is consistent with known conformational changes that result in activation of the repressor for DNA binding. The enzyme−adenylate complex, holoBirA, can either interact with the Biotin Carboxyl Carrier Protein subunit (apoBCCP) of acetyl CoA carboxylase, which results in biotin transfer to apoBCCP. Alternatively, holoBirA dimerizes and binds sequence-specifically to the biotin operator, bioO. The rates and equilibrium constants governing many of the steps in this regulatory system have been measured. The values of these constants are $k_{cat(bio-5'-AMP)} = 0.6$ ($\pm$0.3) s^{-1} (*23*), $k_{on(bio-5'-AMP)} = 5.9$ ($\pm$0.8) $\times$ 10^6 M^{-1} s^{-1} (*23*, *24*), $k_{off(bio-5'-AMP)} = 2.7$ ($\pm$0.3) $\times$ 10^{-4} s^{-1} (*23*, *24*), K_{DIM}(holoBirA dimerization) = 9 ($\pm$0.1) $\times$ 10^{-6} M (*11*), $k_{cat(biotin\ transfer)} = 0.24 \pm 0.01$ s^{-1} (*20*), $k_{on(bioO)} = 10$ ($\pm$1) $\times$ 10^7 M^{-1} s^{-1} (*17*), and $k_{off(bioO)} = 1.7$ ($\pm$0.2) $\times$ 10^{-3} s^{-1} (*17*).

† Supported by NIH Grant R01-GM46511.

* Corresponding author. E-mail, dbeckett@mail.umd.edu; phone, 301-405-1812; fax, 301-314-9121.

10.1021/bi052599r CCC: $33.50
Published on Web 04/27/2006

(ACC), and for repression of transcription initiation at the biotin-biosynthetic operon (*4*, *5*). Since ACC catalyzes the first committed step of fatty acid biosynthesis, covalent attachment of biotin is essential both for ACC function and cellular viability. Post-translational biotin addition occurs in two steps in which biotin is first converted to an activated form, biotinoyl-5′-adenylate (bio-5′-AMP) by transfer of the AMP moiety from ATP (*6*). In the second step, the biotin is transferred from the adenylate to the ϵ amino group of a single lysine residue of the Biotin Carboxyl Carrier Protein (BCCP) subunit of ACC. The adenylate-bound repressor/enzyme or holoBirA serves a second function in which it binds site-specifically to the 40 base-pair biotin operator site, bioO, to repress transcription initiation at the two promoters of the biotin biosynthetic operon (*5*, *7*). Bio-5′-AMP is required for high-affinity binding of the repressor to bioO (*8*). Thus, this small molecule serves both as the intermediate in enzymatic transfer of biotin to apoBCCP and as the allosteric activator of DNA binding. The bifunctionality of biotin protein ligases is conserved in a wide range of eubacteria and archaea (*9*).

Combined *in vivo*, structural, and solution measurements have provided information to formulate a model for functional switching of the biotin repressor. First, *in vivo* measurements indicate that overexpression of the biotin acceptor protein in *E. coli* leads to derepression of transcription initiation at the biotin biosynthetic operon control region (*10*). This indicates that BirA function responds to the intracellular level of the biotin acceptor protein, not biotin. Solution studies of the mechanism of allosteric activation of BirA by the small ligand, bio-5′-AMP, indicate that it functions by promoting repressor dimerization (*11*, *12*). Moreover, this dimerization is important for binding of holoBirA to bioO. Mutations that cause defects in repressor dimerization result in loss of repression activity *in vivo* and a lower affinity of the repressor for the biotin operator *in vitro* (*5*, *13*). Finally, X-ray crystallographic, modeling, and biochemical studies suggest that the homodimer interface that is significant for DNA binding and the heterodimer interface that is utilized for the biotin transfer reaction employ the same surface of BirA, Figure 2 (*14*, *15*). Thus, the two protein−protein interactions are proposed to be mutually exclusive. It should be emphasized that the structure of the heterodimeric complex of apoBCCP bound to holoBirA, while supported by biochemical data (*14*−*16*), is a model that is the subject of ongoing experimental testing. The accumulated results are consistent with the hypothesis that biotin repressor function reflects partitioning of the holorepressor monomer between formation of homodimeric and heterodimeric protein−protein interfaces. Homodimerization results in bioO binding and transcription repression, and heterodimerization results in enzymatic transfer of biotin to the apoBCCP subunit of ACC. While this hypothesis provides a structural basis for the BirA functional switch, it provides no information about the mechanism of the process. One possibility is that BirA function is simply determined by the relative kinetics of formation of the two distinct protein−protein complexes.

This kinetic partitioning model for functional switching of BirA is accompanied by several predictions about the kinetic properties of the biotin regulatory system. First, the key intermediate in the switch, the holoBirA monomer, must

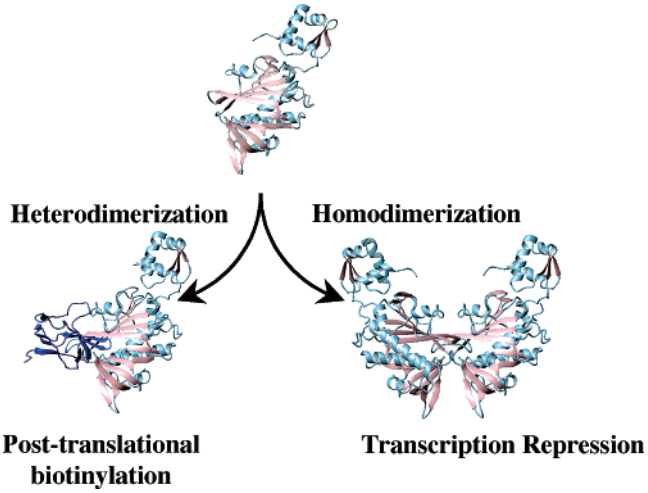

FIGURE 2: Structural models for partitioning of the biotin repressor (holoBirA) between biotin transfer and transcription repression. Holorepressor heterodimerization with apoBCCP results in biotin transfer, and homodimerization leads to bioO binding and transcription repression. The models were constructed using the program MolMol (*30*) with input files 1BIB (BirA monomer), 1HXD (BirA homodimer), and 1K67 (a hypothetical model of the apoBCCP87−BirA heterodimer).

be sufficiently long-lived so that it is available to function in either DNA binding or biotin transfer. As indicated in Figure 1, while synthesis of the adenylate from biotin and ATP is rapid, the resulting adenylate is very tightly bound to BirA and the half-life of the holoBirA complex is 30 minutes. Second, the kinetically active species in bioO binding must be the holoBirA homodimer. Indeed, results of direct kinetic measurements of bioO binding by holoBirA indicate that the dimer is the intermediate species in the assembly of the holoBirA−bioO complex (*17*). A third prediction of the model is that the presence of apoBCCP should not influence the dissociation kinetics of the holo-$BirA_2$−bioO complex. In other words, the switch does not involve active or forced dissociation of the complex by apoBCCP (*17*). Direct measurements of dissociation of the protein−DNA complex indicate that this prediction is also correct. The final prediction of the model is that the initial kinetics of association of holoBirA with bioO should be inhibited by apoBCCP in a manner consistent with inhibition of homodimerization.

In this work, the kinetic partitioning model, which is based, in large part, on the hypothesized structure of the holoBirA−apoBCCP complex (Figure 2), has been tested by measuring the effect of the presence of apoBCCP on the initial rate of holoBirA binding to bioO. The measurements were performed using both standard and rapid quench-flow DNaseI footprinting techniques. The results indicate that, in the presence of apoBCCP, the final equilibrium occupancy of bioO in kinetic time courses decreases in a manner that is dependent on acceptor protein concentration. Neither the biphasic kinetic behavior previously reported nor the rates of the two phases are greatly perturbed by the presence of acceptor protein. Measurements of the dependence of inhibition of bioO binding on apoBCCP concentration reveal that the equilibrium constants for the hetero- and homodimerization of repressor are similar in magnitude. Finally, results of combined MALDI-TOF mass spectrometry and DNaseI footprinting indicate that the recovery of the bioO footprint

in mixtures in which apoBCCP initially fully inhibits bioO binding by holoBirA mirrors the kinetics of BirA-catalyzed biotin transfer to the acceptor protein. These results support a model in which the properties of a multifunctional transcription factor are determined simply by the relative kinetic probabilities of formation of alternative protein−protein interactions. The results also provide indirect support for the hypothesized structure of the holoBirA−apoBCCP complex.

MATERIALS AND METHODS

Chemicals and Biochemicals. The Klenow fragment of DNA polymerase I and restriction enzymes *Hin*d III and *Pst* I were purchased from Promega. The α^{32}P dATP and dGTP used in DNA radiolabeling were obtained from GE Healthcare and the d-biotin, ATP, and DNaseI used in footprinting experiments were from Sigma-Aldrich. The bio-5′-AMP was synthesized using modification of a published protocol (*6*, *18*). All other chemicals used in the preparation of buffers were reagent or analytical grade. The biotin repressor was purified as previously described (*19*). The truncated biotin carboxyl carrier protein (apoBCCP87) was purified as described in Nenortas and Beckett (*20*), with the exception that an additional chromatography step on Hydroxy-apatite ULTROL (PALL) was included to remove trace amounts of the DNaseI introduced in the original purification protocol. This C-terminal domain fragment of BCCP has been shown to function identically to the intact protein in the biotin transfer reaction (*20*).

Preparation of DNA for Footprinting. The plasmid pBioZ was digested with *Hin*d III, and the purified, linearized DNA was labeled with α-^{32}P dATP and dGTP or filled in with cold dNTPs for biotinylation studies using Klenow fragment (*18*, *21*). All DNA was purified over an Elutip column (Scheicher & Schuell), phenol/chloroform-extracted, ethanol-precipitated, and digested with *Pst* I. The desired restriction fragment was isolated by electrophoresis on a 1% agarose gel, recovered by electroelution (*21*), and purified over an Elutip column. Precipitated, radiolabeled DNA was resuspended to a final concentration of approximately 20 000 cpm/μL in TE buffer and stored at 4 °C and cold DNA resuspended in TE to a final concentration of 8×10^{-3} pmol/μL.

Quench-Flow DNaseI Footprinting. Quench-flow footprints were performed using modifications of the methods outlined by Hsieh and Brenowitz (*22*). The reaction buffer used contained 10 mM Tris-HCl, pH 7.5, at 20 °C, 200 mM KCl, 2.5 mM $MgCl_2$, 1 mM $CaCl_2$, 2 μg/mL sonicated calf thymus DNA, and 100 μg/mL BSA. The biotin was always present at a concentration in excess of the final BCCP87 concentration, and the ATP concentration was either 0.5 or 1.0 mM. BirA is known to be saturated with bio-5′-AMP under these conditions (*23*, *24*). A 500 μL BirA solution at twice the desired final experimental concentration and two separate solutions containing labeled DNA diluted into reaction buffer to each yield 300 μL of a 2000 cpm/mL solution were prepared. While one DNA solution contained apoBCCP87 at twice the final desired concentration, the second control solution contained no acceptor protein. The final DNA fragment concentration in each of these solutions was approximately 4×10^{-10} M. All solutions were preequilibrated at 20 °C for 20 min. A 0.07 mg/mL DNaseI solution used for digestions was prepared by dilution of a 20 mg/mL stock solution in DNaseI Storage Buffer (*25*) into wash buffer containing 10 mM Tris-HCl, pH 7.5, at 20 °C, 200 mM KCl, 2.5 mM $MgCl_2$, and 1 mM $CaCl_2$ immediately prior to use. Quench-flow DNaseI footprinting reactions were performed using a Kintek Chemical Quench-Flow, model RQF-3, and reactions were treated as previously described (*17*).

Dependence of BioO Occupancy on [apoBCCP87]. DNaseI footprinting was used to probe the effect of increasing [apoBCCP87] on the equilibrium level of bioO occupancy by holoBirA. In these measurements, mixing was performed for only 60−100 s prior to addition of the cleavage enzyme. For all reactions, buffer contained 10 mM Tris-HCl, pH 7.5, at 20 °C, 200 mM KCl, 2.5 mM $MgCl_2$, 1 mM $CaCl_2$, 2 μg/mL sonicated calf thymus DNA, 100 μg/mL BSA, 800 μM biotin, and 1 mM ATP. A range of apoBCCP87 dilutions, the concentrations of which were guided by simulations of the inhibition curves discussed in Results, were combined in this buffer with 12 000 cpm labeled bioO DNA (total volume = 45 μL). Reactions were initiated by addition of 5 μL of holoBirA, bringing each sample to its final desired concentrations of both proteins. After an incubation of the appropriate duration, 5 μL of 0.0055 mg/mL DNaseI was added to each reaction followed by a 20 s digestion and quenching with 33 μL of 50 mM Na_2EDTA. The reactions were precipitated with 700 μL of 0.4 M NH_4-OAc and 0.1 mg/mL tRNA in absolute ethanol and treated as previously described (*17*).

Long Time-Scale Footprinting. Long time-scale experiments were performed over the course of 7 h to monitor the development of DNaseI footprints with time in the presence of apoBCCP87. An experimental reaction containing 350 μM bio-5′-AMP in 10 mM Tris-HCl, pH 7.5 at 20 °C, 200 mM KCl, 2.5 mM $MgCl_2$, 1 mM $CaCl_2$, 2 μg/mL sonicated calf thymus DNA, and 100 μg/mL BSA; labeled DNA sufficient to yield 12 000cpm/reaction; and 303.2 μM BCCP87 was mixed, and a 50 μL aliquot was removed to serve as the −BirA control. Reactions were preequilibrated at 20 °C for 20 min. At $t = 0$, a small volume of holoBirA was added to the reaction bringing its final concentration to 8.5×10^{-8}M and apoBCCP87 to 300 μM. At appropriate intervals, the reaction was mixed and a 50 μL aliquot transferred to a new eppendorf tube, to which 5 μL of a 0.0045 mg/mL DNaseI solution, freshly diluted for each time point, was added. The 30 s digestion was stopped by quenching with 33 μL of 50 mM Na_2EDTA, and the reactions were precipitated with 700 μL of 0.4 M NH_4OAc and 0.1 mg/mL tRNA in absolute ethanol and treated as previously described (*17*).

Data Analysis. Footprinting gels were dried, and images were produced by 40 h exposures of the gels to storage phosphor screens and digitized using a Molecular Dynamics Storm phosphorimaging system (GE Healthcare). In analysis of each kinetic footprint, the optical densities of a subset of the bands representing the bioO operator site were integrated and progress curves were generated as described by Hsieh and Brenowitz (*22*). All progress curves for association of holoBirA with bioO were initially subjected to nonlinear least-squares analysis using the program Origin7. Since the protein concentration utilized in each reaction was always much greater than the DNA concentration, the pseudo-first-

order approximation applies and the free holoBirA concentration is equivalent to its total concentration. Data from progress curves were analyzed using a double exponential model:

$$\bar{Y} = A_1(1 - e^{-k_{1obs}t}) + A_2(1 - e^{-k_{2obs}t})$$

where $\bar{Y}$ is the fractional saturation of the operator site, k_{1obs} and k_{2obs} are the observed rates of the two kinetic phases, and A_1 and A_2 are the amplitudes of the two phases. In general, the addition of apoBCCP87 to the reactions was found to primarily decrease the amplitudes of the two phases. The Chi-squared value and the distribution of residuals were used in assessing the quality of all fits.

The fractional saturation of operator by repressor at equilibrium was determined as a function of apoBCCP87 concentration. All measurements of operator occupancy were made at short mixing times of 60 or 100 s. In equilibrium footprints, the fractional saturation of the operator is 1.0 at the holoBirA concentrations used in the footprints. Thus, the fractional occupancies for the samples obtained in the presence of apoBCCP87 were normalized relative to the value of 1.0 obtained in the absence of acceptor protein. This is justified by the fact that in all experiments time courses were obtained in parallel in the absence and presence of apoBCCP87. The inhibition curves were analyzed using the program Prism (GraphPad) to obtain the upper and lower plateaus in the curves as well as the equilibrium constant governing the interaction of holoBirA with apoBCCP. The model used in this analysis is discussed in Results.

Mass Spectrometric Measurements of ApoBCCP87 Biotinylation. Mass spectrometric measurements were performed as described previously by Nenortas and Beckett (*20*) with the following changes. An Axima CFR instrument (Shimadzu) was used to weigh the BCCP87. Reactions containing 300 μM BCCP87, BirA at 8.5×10^{-8} M, 1.33×10^{-4} pmol/μL bioO, and 350 μM bio-5′-AMP in 10 mM Tris, pH 7.50 $\pm$ 0.02, at 20 °C, 200 mM KCl, and 2.5 mM $MgCl_2$ in a total volume of 50 μL were incubated at 20 °C. At indicated times, the reaction was mixed and 5 μL aliquots were removed and immediately lyophilized. Samples were reconstituted in 0.1% trifluoroacetic acid in water to a final concentration of 50 pmol/μL, desalted with a ZipTipC18 (Millipore), eluted in 50 mM α-cyano-4-hydroxycinnamic acid in 70% acetonitrile/30% 0.1% TFA in water, and spotted in 0.5 μL aliquots onto the target. Bovine insulin and horse heart cytochrome *c* (Sigma-Aldrich) were used as calibrants at their known protonated masses. The percentage of unbiotinylated BCCP87 remaining at each time point was calculated by dividing the intensity of the peak for unbiotinylated protein by the sum of the intensities of the peaks for apoBCCP87 and holoBCCP87multiplied by 100. Results of control experiments in which mixtures of known ratios of apo- and holoBCCP87 were subjected to MALDI-TOF MS indicate a correlation between the measured fraction of apospecies and the input value and, thus, justify this method of quantitation of the time course of biotin transfer (data not shown).

RESULTS

ApoBCCP87 Inhibits the Initial Kinetics of HoloBirA Binding to BioO. The initial kinetics of holoBirA binding to bioO have previously been measured using rapid quench-flow DNaseI footprinting, and the experimental design used for those measurements is shown in Figure 3a (*17*). The difference between the competition measurements and the simple kinetic measurements of holoBirA binding is that, in addition to the bioO DNA fragment, the reactant line/syringe on the left side of the mixing apparatus (Figure 3a) also contains apoBCCP87, the C-terminal domain fragment of the Biotin Carboxyl Carrier Protein subunit of acetyl CoA carboxylase. This fragment has been previously shown to be identical to the intact subunit in the biotin transfer reaction (*20*). Thus, upon mixing the two reactant solutions, holoBirA has the opportunity to interact with either bioO DNA or apoBCCP87.

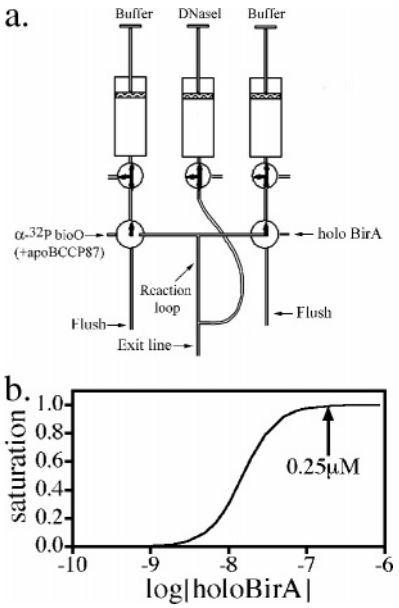

FIGURE 3: Inhibition of repressor binding to bioO by apoBCCP87 (a) Experimental design: The radiolabeled bioO DNA in the absence or presence of apoBCCP87 is rapidly mixed with the holoBirA in the reaction loop. Occupancy is probed by addition of DNaseI from the indicated line, and reactions are quenched by expulsion through the exit line into a solution containing EDTA. (b) The initial holoBirA concentration utilized in inhibition studies indicated on a simulated equilibrium curve for repressor binding to bioO. The curve was simulated using a model in which repressor dimerization is coupled to bioO binding with parameters obtained previously (*11*, *12*).

The holoBirA concentration used in the competition measurement must be carefully chosen. This is because, while the reference or −apoBCCP87 signal must be sufficiently large to enable detection of perturbation resulting from addition of the acceptor, the system must also be poised for perturbation. A simulated equilibrium titration curve of bioO with holoBirA is shown in Figure 3b. When this curve is used as a guide, the holoBirA concentration initially chosen for the competition measurement is 2.5×10^{-7} M because, while it is sufficient for saturation of bioO, it is also close to the transition region of the equilibrium binding curve.

Time-resolved footprints obtained with and without 300 μM apoBCCP87 are shown in Figure 4a. Qualitatively, the footprints obtained in the two conditions are very different. While the evolution of the control footprint (−apoBCCP87) is apparent in the gel image, it is difficult to detect the footprint in the presence of the acceptor even at the longest mixing time of 40 s. The normalized time courses for

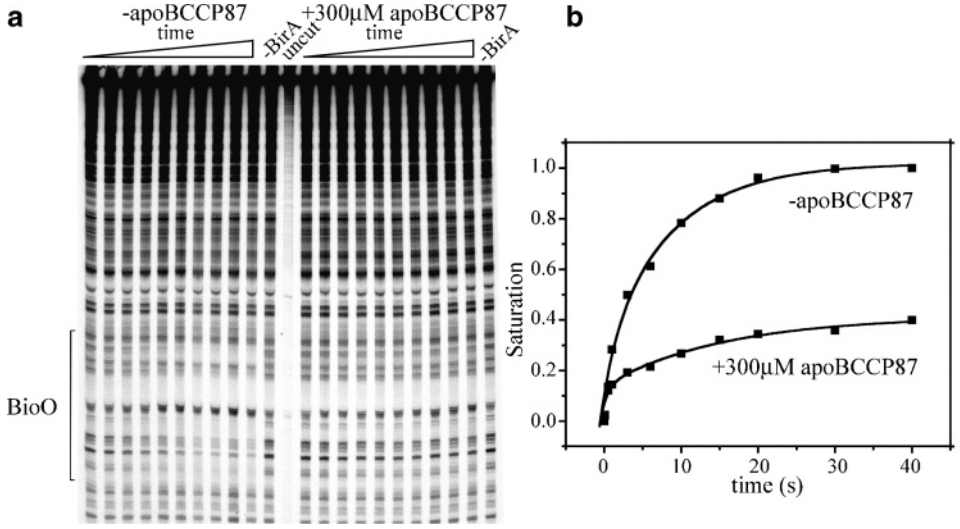

FIGURE 4: (a) Time-resolved DNaseI footprints obtained in the absence and presence of 300 μM apoBCCP87; (b) Time courses of bioO binding in the presence and absence of apoBCCP87. The solid lines represent the best-fit curves simulated using parameters obtained from nonlinear least-squares analysis of the kinetic data to a double-exponential model.

operator binding obtained from quantitation of the footprint data are shown in Figure 4b. Consistent with previously published results, the time course of repressor binding in the absence of apoBCCP87 is biphasic. Results of data analysis from 11 measurements of this time course indicate apparent rates of 2 ± 3 and 0.14 ± 0.09 s^{-1} for the fast and slow phases, respectively. In the presence of apoBCCP87, the time course of holoBirA binding to bioO is also well-described by a double-exponential model. However, the total change in bioO saturation over the time course is approximately one-half of that obtained in the absence of acceptor protein. The rates of the two phases measured in the presence of 300 μM apoBCCP87 are 2 ± 3 and 0.11 ± 0.02 s^{-1} for the fast and slow phases, respectively.

Interpretation of the inhibition of the holoBirA-bioO binding kinetics by apoBCCP87 requires knowledge of the modification state of the acceptor protein once the DNA binding process has reached equilibrium. This is because once the heterodimeric complex forms between holoBirA and apoBCCP87 biotin can be transferred to the acceptor protein. Significant conversion of apoBCCP87 to the biotinylated form will render interpretation of the inhibition measurements difficult. Reactions were carried out under conditions similar to those used for the footprinting reactions, and the resulting samples were subjected to MALDI-TOF mass spectroscopic analysis. The results indicate that little to no biotinylation occurs in the 40 s time frame utilized for the kinetic measurements (see below).

The Affinity of HoloBirA for ApoBCCP87. To obtain quantitative information about the inhibition of bioO binding by apoBCCP87, time courses were measured at a single holoBirA and multiple apoBCCP87 concentrations (Figure 5). As apoBCCP87 concentration is increased from 10−500 μM, the time courses remain biphasic. However, the final level of bioO saturation with holoBirA in each time course decreases as acceptor protein concentration is increased. Moreover, consistent with the results observed in the presence of 300 μM acceptor protein, the rate of the fast phase is similar in the presence and absence of acceptor protein, with rates ranging from 2 ± 2 to 5 ± 5 s^{-1}. Moreover, at 500 μM apoBCCP87, the rate of the slow phase

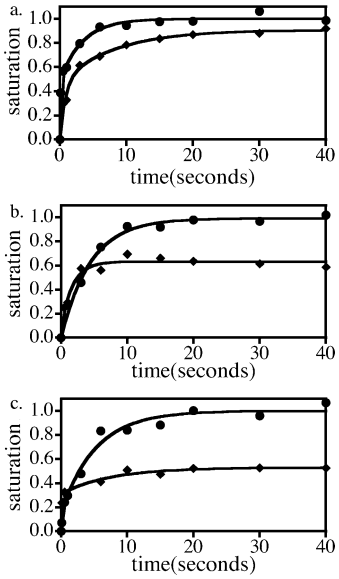

FIGURE 5: Time courses of bioO binding obtained in the absence (●) and presence (♦) of apoBCCP87; [holoBirA] (monomer) = 2.5×10^{-7} M, [apoBCCP87] is 10 μM (a), 200 μM (b), 500 μM (c). The solid lines represent simulations of the curves using the best-fit parameters obtained from data analysis using a double-exponential model for the time course.

is only decreased to approximately one-half of that measured in the absence of acceptor protein. Significantly, at the holoBirA concentration of 2.5×10^{-7} M used in these measurements, the maximum inhibition of bioO binding at equilibrium is approximately 50%.

The dependence of bioO binding kinetics on apoBCCP87 concentration can be used to obtain information about the affinity of the acceptor protein for holoBirA. As indicated above, the major effect of increasing apoBCCP87 concentration is a decreased level of bioO saturation by holoBirA when the system has reached equilibrium. This is consistent with the idea that apoBCCP87 inhibits bioO binding by sequestering holoBirA in a heterodimeric complex. While this effect was measured in kinetic time courses, the observed decrease in the final equilibrium level can be treated using the equilibrium relationship between occupancy of bioO and

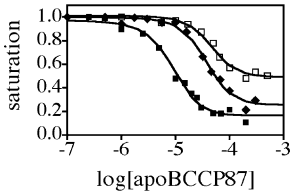

FIGURE 6: Inhibition of the equilibrium saturation of bioO by holoBirA increases with increasing apoBCCP87 concentration. The data curves represent measurements obtained at three holoBirA monomer concentrations of 8.5×10^{-8} M (■), 1.47×10^{-7} M (◇), and 2.5×10^{-7} M (□). The solid curves represent the best fits of the data to the model provided in eq 3.

holoBirA and apoBCCP87 concentrations. As indicated in Figure 1, binding of holoBirA to bioO is coupled to dimerization. Thus, fractional saturation of bioO with holoBirA in the absence of acceptor protein is provided by the following expression:

$$\bar{Y} = \frac{K_{\text{bioO}} K_{\text{DIM}} [\text{holoBirA}]^2}{1 + K_{\text{bioO}} K_{\text{DIM}} [\text{holoBirA}]^2} \quad (2)$$

where $\bar{Y}$ is the fractional saturation of bioO with holoBirA, K_{bioO} is the equilibrium association constant governing the interaction of the holoBirA dimer with bioO, and K_{DIM} is the equilibrium association constant governing dimerization of holoBirA. A modification of this simple binding relationship is sufficient to model the effect of added acceptor protein on the equilibrium level of occupancy of bioO by repressor. In the competition experiments, the fractional occupancy of bioO is perturbed by interaction of some fraction of holoBirA with apoBCCP87. Since apoBCCP87 forms a 1:1 complex with holoBirA (*20*), the modified form of eq 2 that describes the inhibition is:

$$\bar{Y} = \frac{K_{\text{bioO}} K_{\text{DIM}} \left([\text{holoBirA}] \left(1 - \frac{K_{\text{I}} [\text{apoBCCP}]}{1 + K_{\text{I}} [\text{apoBCCP}]} \right) \right)^2}{1 + K_{\text{bioO}} K_{\text{DIM}} \left([\text{holoBirA}] \left(1 - \frac{K_{\text{I}} [\text{apoBCCP}]}{1 + K_{\text{I}} [\text{apoBCCP}]} \right) \right)^2} \quad (3)$$

As this expression indicates, the holoBirA concentration is perturbed to an extent directly related to its fractional saturation with apoBCCP87. In turn, fractional saturation of holoBirA by acceptor protein is determined by an inhibition constant governing the heterodimeric interaction, K_{I}, as well as the apoBCCP87 concentration. The validity of this relationship requires that within the time frame of the kinetic inhibition measurements little or no apoBCCP87 is converted to the holo-form, which results of MALDI-TOF mass spectrometry confirm (see below).

The apoBCCP87 concentration dependence of fractional saturation of bioO by holoBirA at equilibrium is shown in Figure 6. The data were analyzed using the model shown in eq 3. In the analysis, the parameters K_{bioO}, and K_{DIM} are fixed at known measured values (*11*, *12*, *19*), and the holoBirA and apoBCCP87 concentrations are assumed to be equal to their total concentrations. The only unknown parameters are the equilibrium association constant governing the apo BCCP87−holoBirA interaction and the upper and lower plateaus in the inhibition curve. The analysis yields an inhibition constant, K_{I}, of 3.4 ± 0.2 μM. Simulations of apoBCCP87 inhibition curves at different total holoBirA concentrations predict that the position of the curve on the log[apoBCCP87] scale should depend on the initial repressor concentration and that lower concentrations of acceptor protein should be required to compete out bioO binding as the total holoBirA concentration is decreased. Results of the experimental test of this prediction are shown in Figure 6. These results illustrate two points. First, consistent with the simulations, the position of the curve on the log[apoBCCP87] curve depends on the initial holoBirA concentration. A second feature of the results is that the lower plateau in the inhibition curve decreases with decreasing holoBirA concentration. The data were analyzed using eq 3 to obtain the equilibrium constant for the heterodimeric protein−protein interaction. In these analyses, the upper and lower plateaus were also treated as adjustable parameters. The result of this analysis of all three curves yields an average K_{I} for the apoBCCP−holoBirA interaction of 2.8 ± 0.4 μM.

Control of BioO Binding by Apo-Acceptor Protein Concentration. In the cell, the biotin repressor switches from its function in transcription repression to post-translational biotin addition in response to the intracellular biotin demand. Increased demand is signaled by an increase in intracellular acceptor protein concentration (*10*). As the pool of apoBCCP decreases, the free holoBirA concentration is predicted to increase, thereby increasing the occupancy of the biotin operator sequence. Thus, in the competition experiments, as the apoBCCP87 is converted to its holo-form, holoBirA should become available to dimerize and bind to the bioO. This prediction is based on the assumption that the accumulating holoBCCP87 does not interact with holoBirA, an assumption that is found to be correct (data not shown). To test this prediction, the holoBirA and apoBCCP were first combined at concentrations in which bioO binding was completely inhibited. The time dependencies of the conversion of apoBCCP to its holo-form and the operator site from its free to fully occupied state were measured using MALDI-TOF mass spectrometry and DNaseI footprinting, respectively.

The time course of apoBCCP87 biotinylation by holoBirA was first measured using MALDI-TOF mass spectrometry. The holoBirA and apoBCCP87 concentrations utilized for these measurements were 8.5×10^{-8} M and 300 μM, respectively. While the acceptor protein concentration is much higher than that found *in vivo*, it was used because, as shown in Figure 6, bioO binding is completely inhibited at these levels of the two proteins. Moreover, to avoid the complications for mass spectrometry associated with using biotin and ATP as small molecule substrates for biotinylation, the biotin donor used in these experiments is chemically synthesized bio-5′-AMP. As indicated in Figure 1, this is justified by the long half-life of the holoBirA monomer complex. The time course of biotin transfer measured by MALDI-TOF MS is shown in Figure 7a. These results indicate that complete conversion of apoBCCP87 to its holoform requires approximately 7 h.

The time dependence of appearance of the bioO footprint was measured using conditions identical to those employed for measurements of the biotin-transfer reaction above. In these reactions, bioO binding is initially completely inhibited

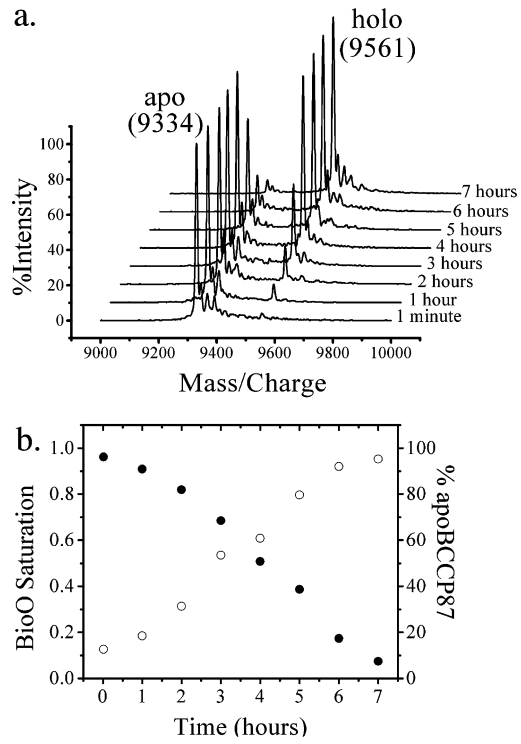

FIGURE 7: Correlation of biotinylation of apoBCCP with evolution of the holoBirA footprint on bioO monitored by MALDI-TOF MS and DNaseI footprinting. (a) Conversion of apoBCCP87 to holoBCCP87 was measured by monitoring the time course of the increase in the mass of the protein from its unbiotinylated to its biotinylated value. (b) Time courses of biotinylation (●) measured by mass spectrometry and the evolution of the bioO footprint (○) measured by DNaseI footprinting.

by apoBCCP87 and the dependence of the operator occupancy on time was probed by cleavage with DNaseI. Results of these measurements are shown in Figure 7b along with the quantitation of the time course of biotin transfer. The time dependence of bioO occupancy by holoBirA directly mirrors the conversion of apoBCCP87 to its holo- or biotinylated form.

DISCUSSION

The *Escherichia coli* Biotin Regulatory System provides an example of the use of a single multifunctional protein for both metabolic and transcription regulatory processes. In related systems for which structural data are available, the emerging theme is that the specific protein partner of the multifunctional protein dictates function. For example, while in its role in adherens junctions β-catenin interacts with E-cadherin, as a transcriptional coactivator it binds to transcription factors. These two protein−protein interactions are, moreover, mutually exclusive (*26*, *27*). The structural data on this and related systems provide no information about the mechanism by which partner switching occurs. The work in this paper is designed to test the simple probability of encounter mechanism for the biotin repressor functional switch.

Addition of apoBCCP87 to reactions for measuring the initial kinetics of the holoBirA−bioO interaction reveals that the major effect is a decrease in the final equilibrium level of operator occupancy. This observation is consistent with the idea that, at sufficiently high concentrations, apoBCCP87 preferentially sequesters holoBirA in a heterodimeric complex, thereby reducing the availability of holoBirA for homodimerization and bioO binding. Consequently, final equilibrium levels of bioO saturation are decreased. Given that the rate of any bimolecular association process increases with increasing concentration of the reactants, the most straightforward interpretation of the inhibition of bioO binding is that as acceptor protein concentration is increased heterodimerization is kinetically favored over homodimerization.

Inhibition of the equilibrium occupancy of bioO by holoBirA due to apoBCCP addition is never complete and depends on the total holoBirA concentration present in the competition reaction. As holoBirA concentration is decreased, the maximal inhibition increases. For example, while at 2.5×10^{-7} M holoBirA maximal inhibition is approximately 50%, at 8.5×10^{-8} M repressor, it is 80 to 90%. This suggests that at the higher repressor concentration the kinetics of bioO binding are sufficiently fast that apoBCCP87 is limited in its ability to compete. Consideration of the mechanism of the holoBirA−bioO binding reaction is useful in interpreting this limit on inhibition. As previously shown, the time courses of holoBirA binding to bioO are biphasic at all holoBirA concentrations (*17*). Moreover, the rates of both phases in the association reaction increase with increasing holoBirA concentration. Indeed, at sufficiently high holoBirA concentration, the faster phase in repressor binding is characterized by a rapid burst. The following chemical model is consistent with those observed results:

$$\text{holoBirA}_2 + \text{bioO} \underset{k_{-1}}{\overset{k_1}{\rightleftharpoons}} \text{holoBirA}_2\cdot\text{bioO} \underset{k_{-2}}{\overset{k_2}{\rightleftharpoons}} {}^*\text{holoBirA}_2-\text{bioO} \quad (4)$$

In this model, a preequilibrium between the holo-repressor monomer and dimer is assumed to exist. At relatively high repressor concentrations, the dimer rapidly forms a collision complex with bioO, holoBirA$_2$−bioO, with a rate governed by the constant, k_1, and the repressor dimer concentration. This collision complex can then either partition toward isomerization to form the final complex *holoBirA$_2$−bioO or it can rapidly dissociate to free protein and DNA. The final complex is very stable and is characterized by a half-life of approximately 7.5 min. Thus, no dissociation of the final complex occurs in the time frame of the kinetic measurements of inhibition. At higher holoBirA concentrations, heterodimerization is less likely to compete with the DNA binding because the flux of dimer through the two-step process is very rapid. As the holoBirA concentration is decreased, both a slower forward reaction for repressor dimerization and slower flux of the dimer through the DNA binding reaction result in greater maximal inhibition of bioO binding. Determination of the relationship of the magnitudes of maximal inhibition to holoBirA and apoBCCP concentrations will require direct measurements of the kinetics of the dimerization reactions. In considering the relationship of this observation to the ability of apoBCCP87 to fully inhibit bioO binding *in vivo*, it should be noted that the intracellular BirA concentration is approximately 7×10^{-8} M (*28*).

Measurements of the dependence of the equilibrium level of bioO saturation on apoBCCP87 concentration indicate that the affinities of the holoBirA monomer for itself and for

apoBCCP87 are similar in magnitude. Results of inhibition measurements obtained at three initial holoBirA concentrations indicate an apparent equilibrium dissociation constant for heterodimerization of 2.8 ± 0.4 μM, a value similar in magnitude to the 9 ± 1 μM equilibrium dissociation constant that characterizes the homodimerization process (*19*). These weak protein−protein interactions, particularly the homodimerization of holoBirA, might lead one to question the efficiency with which repression of transcription initiation at the biotin control region can occur. However, as indicated in Figure 1, in assembly of the repression complex, dimerization is coupled to DNA binding and the final holoBirA$_2$−bioO complex is kinetically very stable (*17*). This kinetic stability ensures effective transcription repression at the biotin operon when biotin requirements are low. The similarity in the energetics of the two dimerization processes argues against equilibrium control of the switch. Rather, as the apoBCCP concentration is increased, the bimolecular rate of heterodimerization relative to that of homodimerization is increased, resulting in preferential partitioning of the system toward the enzymatic function.

The observed inhibition of holoBirA binding to bioO by apoBCCP87 provides support for the hypothesized model of the holoBirA−apoBCCP87 complex (Figure 2, (*15*)). In this model, apoBCCP is proposed to heterodimerize with holoBirA in a manner analogous to that utilized by a second holoBirA monomer in the experimentally determined holoBirA dimer structure. Consequently, the two interactions are mutually exclusive and should, therefore, be competitive. Structurally, the two interactions are similar insofar as the dimer partner extends the central β-sheet of the holoBirA monomer. The inhibition studies suggest that the two dimerization interactions are also energetically similar. In considering equilibrium versus kinetic control in the system, these similar energetics support the kinetic option. The structural basis of the similar energetics is not known, and given that the heterodimer structure has yet to be experimentally determined, speculation is premature.

The kinetic partitioning model predicts that, as the apoBCCP pool is depleted by conversion to the biotinylated form, holoBirA should become available for homodimerization and resulting bioO binding. The results of the long time-course experiments support this prediction. In these measurements, conversion of the bioO occupancy from fully inhibited to 100% binding mirrors the conversion of apoBCCP87 from fully unmodified to fully biotinylated. Thus, as substrate protein, apoBCCP, concentration is depleted, holoBirA becomes available for homodimerization and subsequent bioO binding. While these results provide no information about the time scale of the switch *in vivo*, they do reinforce the idea that it is the supply of unbiotinylated protein that regulates binding of the biotin repressor to bioO. The concentrations of holoBirA and apoBCCP87 of 85 nM and 300 μM, respectively, chosen for these measurements allowed observation of the full range of both acceptor protein biotinylation and bioO occupancy by holoBirA. However, as indicated in Figure 5, this acceptor protein concentration is higher than the 100 μM required to fully inhibit holoBirA binding to bioO. *In vivo*, the BCCP concentration has been estimated to be in the micromolar range and increases with increasing growth rate (*10*). Thus, both its concentration and the BirA concentration of 70 nM are in ranges in which occupancy of bioO can be expected to vary from 100% free to 100% saturated. BioO occupancy will depend on apoBCCP concentration, and the bioO DNA can be considered a "sensor" of free holoBirA dimer supply, a supply that is ultimately controlled by the level of acceptor protein.

The biological activities of several multifunctional transcription factors are regulated by the protein partner with which each interacts. For example, β-catenin switches from a role in only cell adhesion in which it interacts with E-cadherin to a second function in transcription activation (*2*). The second function is acquired in response to Wnt signaling, which leads to increased cytoplasmic concentration of β-catenin. The additional β-catenin binds to the Tcf/Lef family of transcription factors to function as a coactivator. Genetic studies of the GAL gene switch in yeast indicate that the two small molecules, galactose and ATP, influence the protein association state of Gal80 and thus its biological function (*29*). In the absence of galactose, Gal80 dimerizes and interacts with the transcription activator, Gal4, to inhibit transcription initiation at target genes. Increased intracellular galactose results in sequestering of Gal80 monomers in a complex with Gal3, thus, allowing transcription activation by Gal4. In both of these switches, increased availability of the regulatory protein, Gal80 or β-catenin, enables the functional switch. However, unlike BirA, the functional switching of these proteins involves nuclear transport. Despite this added complexity, simple equilibrium thermodynamic or kinetic rules may govern the binding partner switching and, therefore, biological function of these proteins. Elucidation of these rules will require detailed solution studies of these multifunctional transcription factors.

REFERENCES

1. Yap, A. S., Brieher, W. M., and Gumbiner, B. M. (1997) Molecular and functional analysis of cadherin-based adherens junctions, *Annu. Rev. Cell Dev. Biol. 13*, 119−146.
2. Polakis, P. (2000) Wnt signaling and cancer, *Genes Dev. 14*, 1837−1851.
3. Ostrovsky de Spicer, P., and Maloy, S. (1993) PutA protein, a membrane-associated flavin dehydrogenase, acts as a redox-dependent transcriptional regulator, *Proc. Natl. Acad. Sci. U.S.A. 90*, 4295−4298.
4. Barker, D. F., and Campbell, A. M. (1981) Genetic and biochemical characterization of the birA gene and its product: evidence for a direct role of biotin holoenzyme synthetase in repression of the biotin operon in *Escherichia coli*, *J. Mol. Biol. 146*, 469−492.
5. Barker, D. F., and Campbell, A. M. (1981) The birA gene of *Escherichia coli* encodes a biotin holoenzyme synthetase, *J. Mol. Biol. 146*, 451−467.
6. Lane, M. D., Rominger, K. L., Young, D. L., and Lynen, F. (1964) The enzymatic synthesis of holotranscarboxylase from apotranscarboxylase and (+)-biotin, *J. Biol. Chem. 239*, 2865−2871.
7. Otsuka, A., and Abelson, J. (1978) The regulatory region of the biotin operon in *Escherichia coli*, *Nature 276*, 689−694.
8. Prakash, O., and Eisenberg, M. A. (1979) Biotinyl 5′-adenylate: corepressor role in the regulation of the biotin genes of *Escherichia coli* K-12, *Proc. Natl. Acad. Sci. U.S.A. 76*, 5592−5595.
9. Rodionov, D. A., Mironov, A. A., and Gelfand, M. S. (2002) Conservation of the biotin regulon and the BirA regulatory signal in Eubacteria and Archaea, *Genome Res. 12*, 1507−1516.
10. Cronan, J. E., Jr. (1988) Expression of the biotin biosynthetic operon of *Escherichia coli* is regulated by the rate of protein biotination, *J. Biol. Chem. 263*, 10332−10336.
11. Eisenstein, E., and Beckett, D. (1999) Dimerization of the *Escherichia coli* biotin repressor: corepressor function in protein assembly, *Biochemistry 38*, 13077−13084.

12. Streaker, E. D., Gupta, A., and Beckett, D. (2002) The biotin repressor: thermodynamic coupling of corepressor binding, protein assembly, and sequence-specific DNA binding, *Biochemistry 41*, 14263−14271.
13. Kwon, K., Streaker, E. D., Ruparelia, S., and Beckett, D. (2000) Multiple disordered loops function in corepressor-induced dimerization of the biotin repressor, *J. Mol. Biol. 304*, 821−833.
14. Polyak, S. W., Chapman-Smith, A., Mulhern, T. D., Cronan, J. E., Jr., and Wallace, J. C. (2001) Mutational analysis of protein substrate presentation in the post-translational attachment of biotin to biotin domains, *J. Biol. Chem. 276*, 3037−3045.
15. Weaver, L. H., Kwon, K., Beckett, D., and Matthews, B. W. (2001) Competing protein:protein interactions are proposed to control the biological switch of the *E. coli* biotin repressor, *Protein Sci. 10*, 2618−2622.
16. Reche, P. A., Howard, M. J., Broadhurst, R. W., and Perham, R. N. (2000) Heteronuclear NMR studies of the specificity of the post-translational modification of biotinyl domains by biotinyl protein ligase, *FEBS Lett. 479*, 93−98.
17. Streaker, E. D., and Beckett, D. (2003) Coupling of protein assembly and DNA binding: biotin repressor dimerization precedes biotin operator binding, *J. Mol. Biol. 325*, 937−948.
18. Abbott, J., and Beckett, D. (1993) Cooperative binding of the *Escherichia coli* repressor of biotin biosynthesis to the biotin operator sequence, *Biochemistry 32*, 9649−9656.
19. Brown, P. H., Cronan, J. E., Grotli, M., and Beckett, D. (2004) The biotin repressor: modulation of allostery by corepressor analogs, *J. Mol. Biol. 337*, 857−869.
20. Nenortas, E., and Beckett, D. (1996) Purification and characterization of intact and truncated forms of the *Escherichia coli* biotin carboxyl carrier subunit of acetyl-CoA carboxylase, *J. Biol. Chem. 271*, 7559−7567.
21. Maniatis, T., Fritsch, E. F., and Sambrook, J. (1982) *Molecular Cloning, A Laboratory Manual*, Cold Spring Harbor, Cold Spring Harbor, New York.
22. Hsieh, M., and Brenowitz, M. (1996) Quantitative kinetics footprinting of protein-DNA association reactions, *Methods Enzymol. 274*, 478−492.
23. Xu, Y., and Beckett, D. (1994) Kinetics of biotinyl-5′-adenylate synthesis catalyzed by the *Escherichia coli* repressor of biotin biosynthesis and the stability of the enzyme−product complex, *Biochemistry 33*, 7354−7360.
24. Xu, Y., Nenortas, E., and Beckett, D. (1995) Evidence for distinct ligand-bound conformational states of the multifunctional *Escherichia coli* repressor of biotin biosynthesis, *Biochemistry 34*, 16624−16631.
25. Brenowitz, M., Senear, D. F., Shea, M. A., and Ackers, G. K. (1986) Quantitative DNase footprint titration: a method for studying protein-DNA interactions, *Methods Enzymol. 130*, 132−181.
26. Graham, T. A., Weaver, C., Mao, F., Kimelman, D., and Xu, W. (2000) Crystal structure of a beta-catenin/Tcf complex, *Cell 103*, 885−896.
27. Huber, A. H., and Weis, W. I. (2001) The structure of the beta-catenin/E-cadherin complex and the molecular basis of diverse ligand recognition by beta-catenin, *Cell 105*, 391−402.
28. Eisenberg, M. A., Prakash, O., and Hsiung, S. C. (1982) Purification and properties of the biotin repressor: a bifunctional protein, *J. Biol. Chem. 257*, 15167−15173.
29. Pilauri, V., Bewley, M., Diep, C., and Hopper, J. (2005) Gal80 dimerization and the yeast GAL gene switch, *Genetics 169*, 1903−1914.
30. Koradi, R., Billeter, M., and Wuthrich, K. (1996) MOLMOL: a program for display and analysis of macromolecular structures, *J. Mol. Graphics 14*, 51−55, 29−32.

BI052599R